CHARACTERIZATION OF THE TENSILE RESPONSE OF STRAIN HARDENING UHPFRC - CHILLON VIADUCTS

Emmanuel Denarié (1), Lionel Sofia (2), Eugen Brühwiler (1)

(1) Division of Maintenance and Safety of Structures (MCS-ENAC), Ecole Polytechnique Fédérale de Lausanne (EPFL), GC A3 435, Station 18, CH-1015 Lausanne, Switzerland.

(2) Construction Materials Laboratory (LMC-STI), Ecole Polytechnique Fédérale de Lausanne (EPFL), MX G 240, Station 12, CH-1015 Lausanne, Switzerland.

Abstract

The tensile response (strength and deformability) of strain hardening UHPFRC needs to be characterized by adequate test and analysis methods. Inverse analysis methods that do not appropriately take into consideration the influence of the UHPFRC softening behavior on its pre-peak response under bending significantly overestimate the UHPFRC strain hardening domain. Further, the determination of the elastic limit from objective methods remains a challenge. An original simple inverse analysis method has been developed which provides new objective criteria for the determination of: (1) the elastic limit, and (2) the strain hardening response of UHPFRC in the relevant pre-peak domain under bending. The paper reports on the major results achieved in this context, with the background and application of these new methods to the characterization of the tensile response of the UHPFRC used for the reinforcement of the Chillon Viaducts (Switzerland) in 2015.

Résumé

La réponse en traction (résistance et déformabilité) des BFUP écrouissants doit être caractérisée par des méthodes d'essai et d'analyse adéquates. Les méthodes d'analyse inverse qui ne prennent pas correctement en considération la contribution du comportement adoucissant sur la réponse pré-pic flexionnelle conduisent à une surestimation importante du domaine écrouissant des BFUP. De plus, la détermination de la limite élastique sur la base de critères objectifs reste un défi. Une méthode simple et originale d'analyse inverse a été développée avec des critères objectifs pour la détermination de: (1) la limite d'élasticité, (2) l'étendue du domaine écrouissant des BFUP, sur la base du domaine pré-pic pertinent, en flexion. Les principaux résultats obtenus dans ce contexte sont présentés, avec les bases et l'application à la caractérisation de la réponse en traction des BFUP utilisés pour le renforcement de la dalle de roulement des viaducs de Chillon (Suisse) en 2015.

1.   INTRODUCTION

The characterization of the tensile response of likely strain hardening UHPFRC mixes aims at the determination of their strength and deformability values for given conditions of preparation (molds, casting, curing): elastic limit f_{Ute}, maximum strength f_{Utu}, maximum hardening deformation ε_{Utu} and modulus of elasticity E_{Ut}. This can be achieved either directly by means of unnotched uniaxial tensile tests, or indirectly by means of unnotched bending tests associated to inverse analysis methods. Reliable tensile tests are challenging for several reasons and require great care: eccentricities with bending effects can dramatically increase the apparent hardening response and decrease the apparent elastic limit by several MPa; fixed boundary conditions are less forgiving for slight eccentricities but lead to the only reliable estimation of the tensile response after cracking as shown by Kanakubo [1].

More generally, the tensile performance of UHPFRC is governed by the action of their fibrous skeleton. In cases of detrimental fiber orientation, local variations of the fiber dosage, insufficient fibrous mix design, or loss of continuity of the fibrous skeleton (casting joints or flux fronts due to casting procedures) this performance can be severely affected, [2-5]. On the contrary, in cases of favorable fiber orientation with respect to principal stresses such as in the case of thin (with respect to fiber length) laboratory specimen, cast in narrow (with respect to fiber length) molds, the material performances are most often an upper bound, far from design conditions. There is thus no absolute and unique uniaxial tensile response for discontinuous fiber reinforced composites such as UHPFRC; only sample "structural" responses which depend on the methodology of casting and curing and the material composition. This now well-known aspect is covered for design among others by conversion factor K according to [6] and by coefficients η_{hu} et η_k according to [7].

Current inverse analysis methods [8-11] most often neglect the influence of the UHPFRC softening behavior on its pre-peak response under bending, and thus significantly overestimate the UHPFRC strain hardening domain, as shown by the comparison of direct tensile test results and inverse analyses for the same material and casting and curing conditions [11,12]. Furthermore, the determination of the elastic limit from objective methods remains a challenge.

An original simplified inverse analysis method has been developed [13], which provides new objective criteria for the determination of: (1) the elastic limit, and (2) the strain hardening response of UHPFRC samples in the relevant pre-peak domain under bending. This paper reports on the major results achieved in this context, with the background, validation from tensile test results and finite element calculations, and application of these new methods to the characterization of the tensile response of the UHPFRC used for the reinforcement of the Chillon Viaducts (Switzerland) in 2015.

2.   EXPERIMENTAL

2.1   Context and overview

The application of strain hardening UHPFRC for the long-lasting protection and reinforcement of existing structures has demonstrated its advantages and feasibility in numerous cases since 2004 in Switzerland and abroad, [14]. The reinforcement of the 2.1 km long Chillon viaducts in Switzerland in 2014/2015, with ongoing AAR and insufficient bending, shear and fatigue resistance of the deck slabs was a major step towards a systematic

large scale industrialization of this technique, [15]. Altogether, 2400 m^3 UHPFRC were cast as a 40 or 50 mm thick layer with average rates of 60 m^3/day, with a special casting machine.

Passive reinforcement was added in the transversal direction all along the bridges length, and over the piers over 1/8 of the span (negative moment zone) along the longitudinal direction. The requirements (average values on specimens cast on site, with the machine) to the UHPFRC (type UA according to [7]) were a strain hardening response with an elastic limit higher than 7 MPa, a ratio $f_{Utu}/f_{Ute} > 1.1$, and a maximum strain hardening deformation > 1.5 ‰. During this site, complete characterization tests were performed to determine the tensile response of the UHPFRC as it is cast in place, with both tensile and bending tests associated to inverse analyses.

2.2 Materials and preparation of specimen

The material used was Ductal® NaG3 Tx developed by Lafarge for this site [16], with 240 kg/m^3 of smooth straight steel fibers 14/0.2 mm. The fresh UHPFRC was highly thixotropic, perfectly suited for the application on slopes up to 7 %, with the casting machine developed by the contractor, Walo Bertschinger AG, for this site. As such, the workability of the fresh mix just out of the mixer, was not adapted to directly cast specimen and it was decided to produce material samples cut out of square plates (700 mm x 700 mm, 35 mm thick) cast directly under the casting machine with the method used for reinforcing the viaducts. Both four point bending and tensile test specimens were prepared. The individual specimens were cut out of the original plates in different directions with respect to the direction of casting (parallel to longitudinal axis of bridge or perpendicular), surfaced to a thickness of 30 mm, cured at 20°C in the lab and tested at 28 days. The reported results are for the specimens prepared during the application of UHPFRC on the second viaduct, in 2015, for which both tensile and bending test results from same castings are available.

2.3 Four-point bending tests

The specimens were strips of 500 x 100 x 30 mm loaded and instrumented according to Figure 1 a), with a span of 420 mm. The displacement rate imposed by the stroke to points (a) and (b) was 0.5 mm/min pre-peak and 5 mm /min post-peak, with a servo-hydraulic testing machine. Mid span deflections and reaction force were recorded at 5 Hz.
For each series six specimens were tested. First, three specimens were tested in a monotonic way, until a deflection of 25 mm to estimate an average of their maximum force. For the three remaining specimens, a two-step procedure was used: (1) three loading/unloading cycles were performed until 25 % of the average force of the first three specimens tested in a monotonic way, (2) the specimens were subsequently loaded in a monotonic way until 25 mm deflection. For these three specimens, the loading/unloading cycles enable an accurate determination of the elastic limit f_{Ute} as follows. For the last loading cycle, for every pair of measured values: force F_i and average midspan deflection δ_i, the apparent secant elastic modulus E_i is determined after equation (2), with l_m : span, b_m : width and h_m : thickness of the specimen). Additionally, the moving average E_{mi} over the last 20 values $\underline{E_i}$ is calculated for every value of deflection δ_i (i ≥ 20). Finally, the current elastic modulus E_i and its moving average are plotted as a function of the average measured deflection δ_i.

The end of the elastic domain corresponds to force F_A from which an irreversible decrease of 1 % of the moving average E_{mi} of the apparent secant elastic modulus is observed. The elastic limit of the material is given by equation (3):

$$E_i = 0.0177 \cdot \frac{F_i}{\delta_i} \cdot \frac{12 \cdot l_m^3}{b_m \cdot h_m^3} \qquad (2) \qquad\qquad f_{Ute} = \frac{F_A \cdot l_m}{b_m \cdot h_m^2} \qquad (3)$$

The apparent elastic modulus E_U of the material is defined as the value of the apparent secant elastic modulus E_{mi} for Force F_A.

The 1% criterion of detection applied on the secant modulus to detect the elastic limit was validated by the analysis of the intrinsic noise of force and deflection measurements, for two distinct laboratories, with a similar aluminum sample subjected to the four-point bending test procedure presented in this paper. The noise on the deflection measurements under stroke control was the most significant and its effect on the apparent secant modulus (raw values) varied between 0.85 % (lab. 1) and 1.84 % (lab. 2), average values of noise at reloading, over 10 cycles. After applying the moving average to the secant modulus, the noise was below 1 % for the two laboratories.

2.4   Uniaxial Tensile tests

The specimen geometry is shown on Figure 1b). The geometry of the transition zones BC, EF, IJ, LM was defined according to Neuber's model [17] to limit stress concentrations. The specimens were instrumented with two sets of two LVDT on two perpendicular planes (XY and XZ after Figure 1b)) along the cross section of the specimen to verify possible eccentricities, with measurement bases $l_{mes,1}$ and $l_{mes,2}$. A systematic check of the differences among the transducers in each pair confirmed that the effects of eccentricities remained negligible (less than 0.2 MPa flexural effect on the tensile stresses) up to the elastic limit at least. The tests were run with an electro mechanical testing machine with fixed/fixed boundary conditions. The displacement rate imposed by the stroke to the specimens was 0.2 mm/min pre peak and 0.4 mm/min post peak. All data were recorded at 5 Hz.
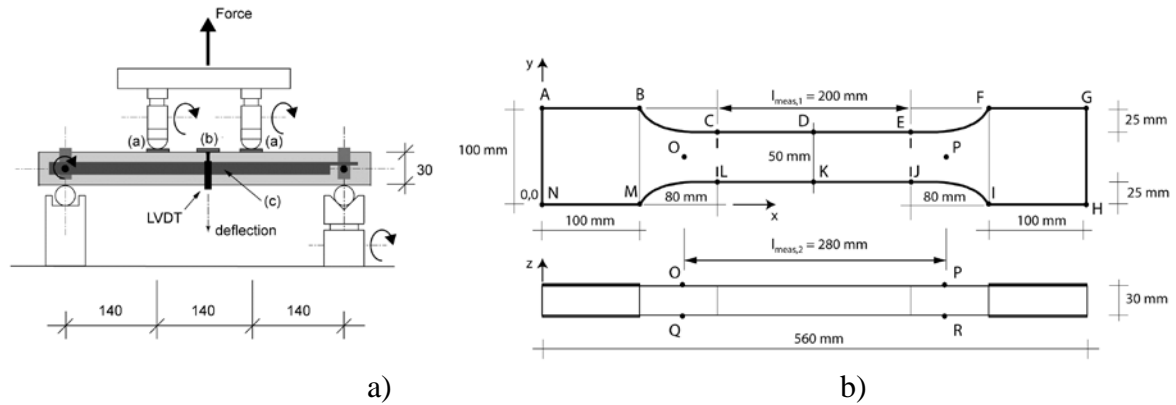

a)   b)

Figure 1: a) four-point bending set-up and specimen, all dimensions in mm, b) tensile test specimen

3.   ANALYTICAL INVERSE ANALYSIS

3.1   Background

A simplified analytical inverse analysis method assuming elastic curvature under 4 point bending of strips, strictly speaking only valid in the elastic domain, was proposed by [6],

Annex 4. It is originally applied only in one point, at the peak, and assumes that the tensile parameters (stress and strain) determined at this point characterize the end of the hardening domain. Consequently, this method neglects the effect of the strain softening response of the material on its pre-peak response under bending and significantly overestimates its hardening response. On the other hand, its formulation is very simple and adapted for a quick inverse analysis, without the need for an iterative procedure.

The same modelling approach was followed with however two improvements: (1) extension of the calculation to the pre-peak domain between points A and C, starting after the elastic limit, up to the peak, according to Figure 2 a), (2) Definition of a limitation criterion to identify point (C) on the Force-deflection response, Figure 2a) at which the softening response of the material enters into play. Following [6, 8], the curvature in the constant moment zone of the specimen is assumed to remain elastic per equation (5), up to the peak force. For a pair of force – mid-span deflection values F_i, δ_i, one gets, with M_i the bending moment, σ_{Uti}, respectively ε_{Uti}, the tensile stress, respectively deformation, at the lower face of the specimen in the constant moment zone, χ_i the curvature in the same zone, α_i the ratio of the height of the « yielding zone » to the specimen height h_m after Figure 2 a), b_m width of the specimen, l_m span, E modulus of elasticity after equation (6) for force F_A:

$$M_i = \frac{F_i \cdot l_m}{6} \qquad (4) \qquad\qquad \chi_i = \frac{216}{23} \cdot \frac{\delta_i}{l_m{}^2} \qquad (5)$$

Equilibrium and compatibility equations in the cross section yield equation (6):

$$2\alpha_i^3 - 3\alpha_i^2 + 1 - \lambda_i = 0 \;\; (6) \qquad\qquad \text{with} \qquad\qquad \lambda_i = \frac{12 \cdot M_i}{b_m \cdot h_m{}^3 \cdot \chi_i \cdot E} \qquad (7)$$

Parameter λ_i can be determined directly from the test results for a series of points evenly spaced in the pre-peak domain, after the elastic limit, between points A and C. Equation (6) can be easily solved using a spreadsheet. Once the values of α_i are known, it is possible to determine the tensile stress and deformation at the lower face of the specimen according to equations (8) and (9), [6], Annex 4.

$$\sigma_{Ut_i} = 0.5(1-\alpha_i)^2 h_m \chi_i E \qquad (8) \qquad\qquad \varepsilon_{Ut_i} = \frac{\sigma_{Ut,i}}{E} + \chi_i \alpha_i h_m \qquad (9)$$
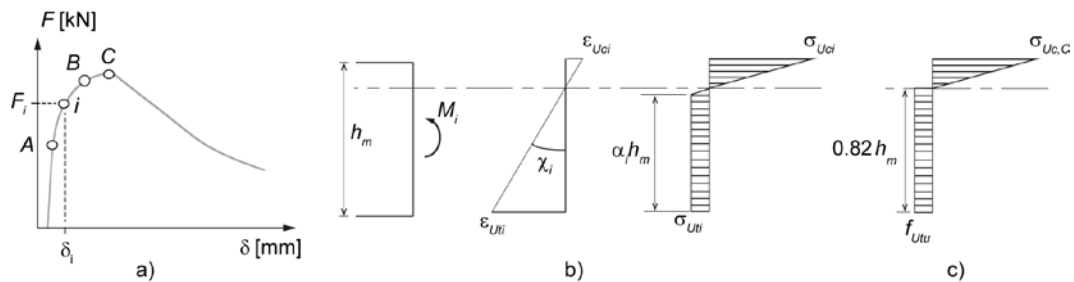

Figure 2: Inverse analysis of four-point bending tests, principles

In order to detect point B according to Figure 2a), after which the softening response of the material comes into play and the inverse analysis method neglecting it is no more valid, an additional criterion linked to the maximum tensile strength of the material f_{Utu} is introduced.

Numerous finite elements simulations [18] for a specimen geometry according to Figure 1a) and strain hardening UHPFRC, have shown that the position of the neutral axis at peak force can be assumed to be $0.82 \cdot h_m$ for strain hardening UHPFRC and specimen geometries according to Figure 1a) (depth 30 ± 2 mm), provided that the compressive stresses remain in the elastic range. Following this assumption, with peak Force F_C and the stress distribution shown on Figure 2 c), yields equation (10):

$$f_{Utu} = 0.383 \cdot \frac{F_C \cdot l_m}{b_m \cdot h_m{}^2} \qquad (10)$$

Thus, the inverse analysis method is performed for a series of points evenly distributed between points A and C. The first point "j" for which the calculated stress σ_{Utj} is larger than the value of f_{Utu} after equation (8) gives an estimate of the strain hardening limit of the UHPFRC, $\varepsilon_{Utu} = \varepsilon_{Utj.}$

The choice of the first point of calculation is done such that the height of the "plastic zone" α_i is at least 0.5, which means $\lambda_i \leq 0.5$, to involve at least a plastic zone equal to 50 % of the cross section of the specimen in the calculation. The total recommended number of points for the method between points A and C is at least 10. A preliminary smoothing of the Force - displacement curve (for instance by means of a moving average) helps avoiding using local minima or maxima from the raw experimental data that could bias the detection of point B.

3.2 Application to the UHPFRC used on the Chillon viaducts site

Table 1 summarizes the tests that were realized in 2015 to characterize the tensile response of the UHPFRC applied on the site. Two independent testing labs were involved, with both tensile and four-point bending tests (4PTB) with specimens cut out of plates cast with the casting machine, in two perpendicular directions.

Table 1: Overview of tests realized for characterizing the tensile properties of the UHPFRC applied on the Chillon viaducts in 2015 (number of specimen)

Laboratory	Series 1 - Parallel to laying direction		Series 2 - Perpendicular to laying direction	
	Tensile test	4 PTB test	Tensile test	4 PTB test
Lab. 1	6 x	6 x	6 x	6 x
Lab. 2		6 x		6 x

The tensile response of the UHPFRC was evaluated indirectly by means of inverse analyses of the 4PTB tests results with: (1) the analytical method described in § 2.3 and 3.1, and (2) a Non Linear Finite Element code (MLS/FEMMASSE) [18]. The bases of the FEM model (Smeared Crack Model with bulk energy dissipation) and verifications of mesh size objectivity are described in [19]. Two specimens of each series were analyzed in details and used for comparison. The results were then compared to those of the uniaxial tensile tests.

Figure 3a) shows the results of test series 1 (4 PTB specimens) with the predictions of the best fits of the FEM models applied to two specimens with different responses. Figure 3b) and c) show the tensile laws obtained by the inverse analysis by FEM. Results from Lab. 2 have significantly more scatter than for those of Lab. 1. This effect can be due to the variability of the casting process and the limited size of the plates from which the specimen

were extracted with respect to the size of the casting machine. However, on average the results show similar trends. A very close fit is achieved with the FEM models. The material exhibits a clear strain hardening response.

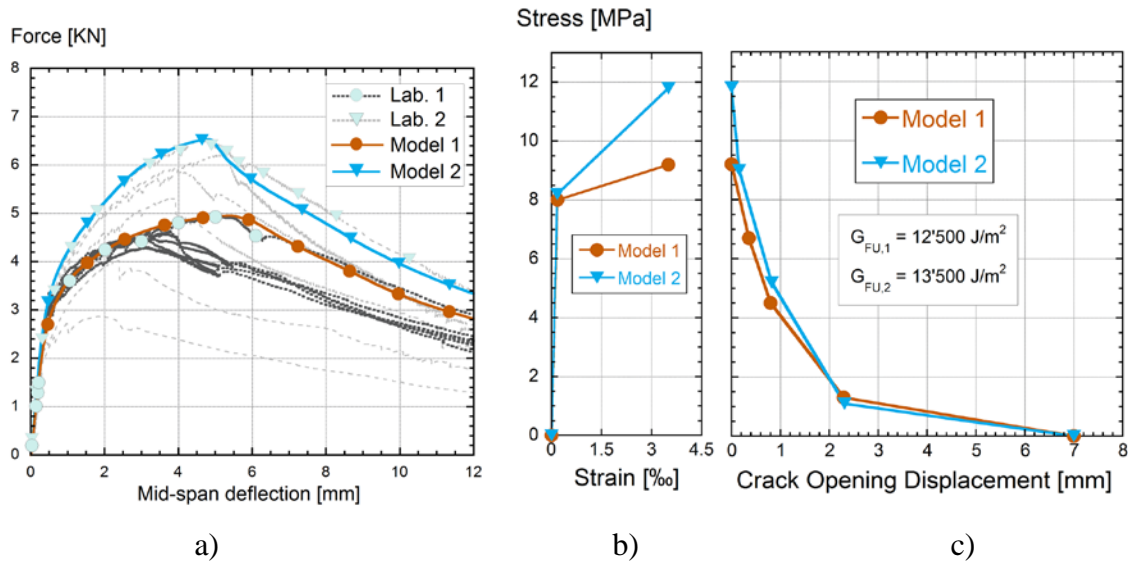a)   b)   c)

Figure 3: a) 4PTB test results, series 1 and best fits of the FEM model, b) FEM model, tensile law: hardening domain, c) FEM model, tensile law: softening domain

Similarly, Figure 4a) shows the results of test series 2 (4 PTB specimens) with the predictions of the best fits of the FEM models applied to two specimens with different responses. Figure 4b) and c) show the tensile laws obtained by the inverse analysis by FEM. Results from Labs 1 and 2 coincide well in terms of average and scatter. The closest fit is achieved with the models with a small strain hardening domain (likely to be microcracking without distributed multiple cracks). For this orientation of the specimens with respect to casting direction, no significant strain hardening response is obtained.

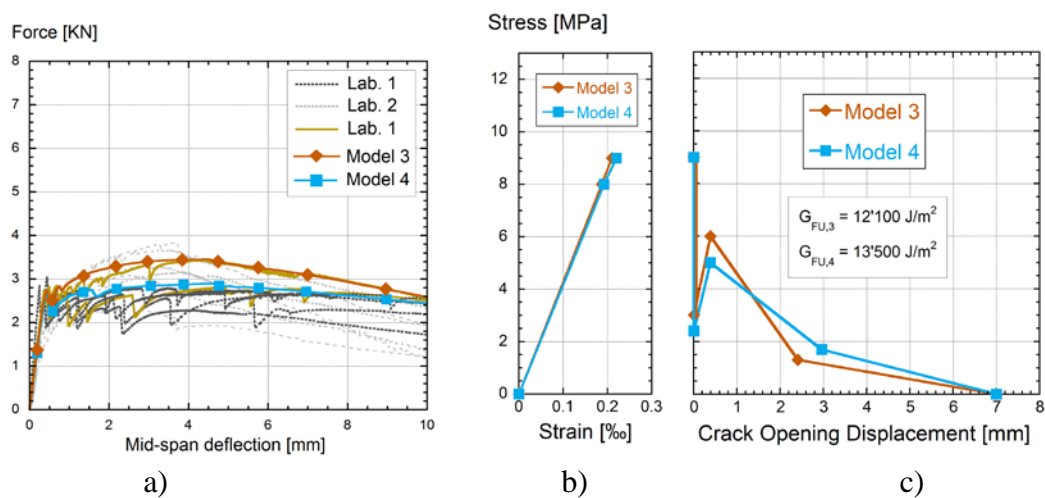a)   b)   c)

Figure 4: a) 4PTB test results, series 2 and best fits of the FEM model, b) FEM model, tensile law: hardening domain, c) FEM model, tensile law: softening domain

Figure 5 shows the evolution of the secant modulus determined according to § 2.3 as a function of the deflection for the specimen fitted by FEM model 1 on Figure 3a). The elastic limit according to the 1 % irreversible decrease criterion is found for a deflection of 0.223 mm, with a value f_{Ute}=7.92 MPa. The corresponding elastic modulus is 43,400 MPa.

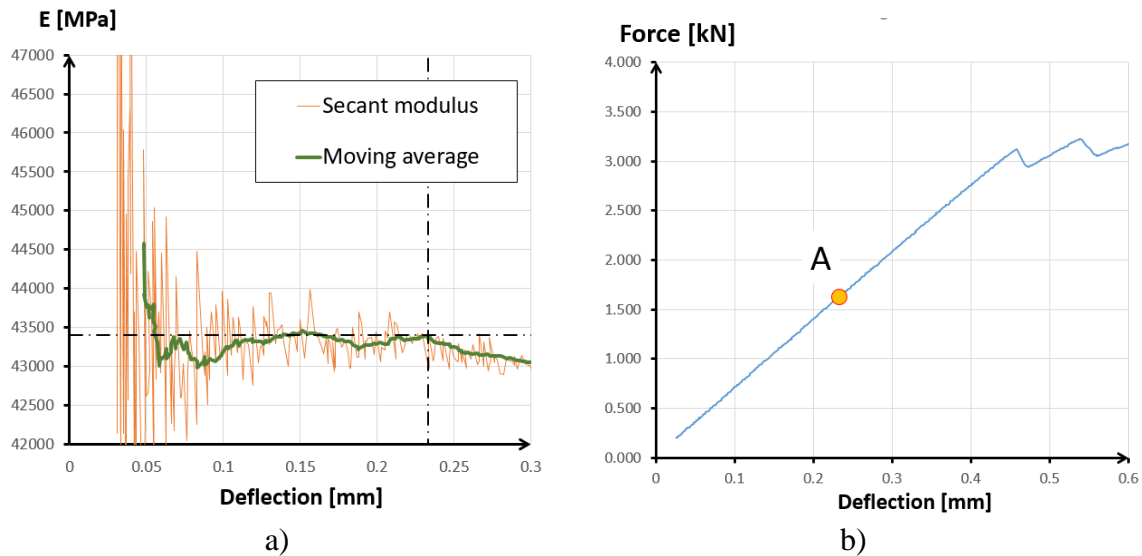a)   b)

Figure 5: a) secant modulus as a function of deflection for the specimen fitted by FEM Model 1, b) position of the elastic limit on the force-deflection curve

Figure 6 illustrates the application of the analytical inverse analysis method (I.A. model A) to the specimen fitted by FEM Model 1 on Figure 3a). The range of hardening predicted by the method as well as the maximum strength correspond very well with the values obtained by fitting with the FEM model 1, for the same specimen.

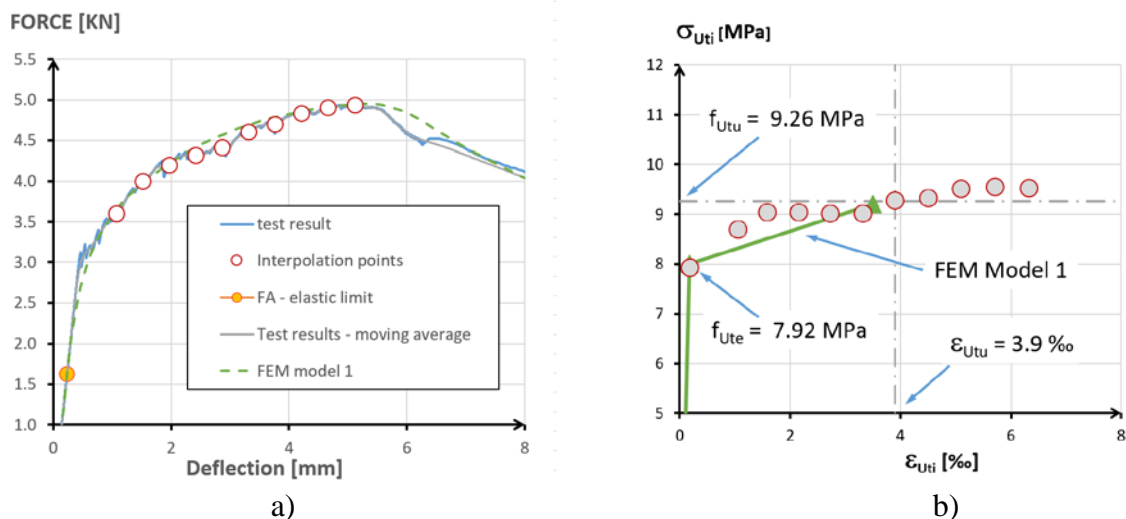a)   b)

Figure 6: example of analytical inverse analysis procedure (I.A. model A): a) test results, interpolation points and fit by FEM model 1, b) tensile properties compared to FEM model 1

Finally, all models are compared to the results of the uniaxial tensile tests on Figure 7. I.A models A and B resp. correspond to FEM Models 1 and 2 fitted on the associated experimental curves according to Figure 3a). Overall, the FEM models and the results from the analytical inverse analysis method correspond very well with each other, and with the observed tensile test results. Contrary to 4PTB test results from both labs, no significant difference can be observed between the two orientations of the specimens with respect to the casting direction for the tensile tests results. This effect could be again explained by the "small "size of the plates (700 x 700 mm) from which the specimens were taken compared to the size of the laying machine (several meters). Indeed, considering all test results from series 1 and 2, both 4PTB and direct tension, the material cast on the Chillon viaducts exhibits a strain hardening response in various orientations, at different places, corresponding to the required strain hardening response.
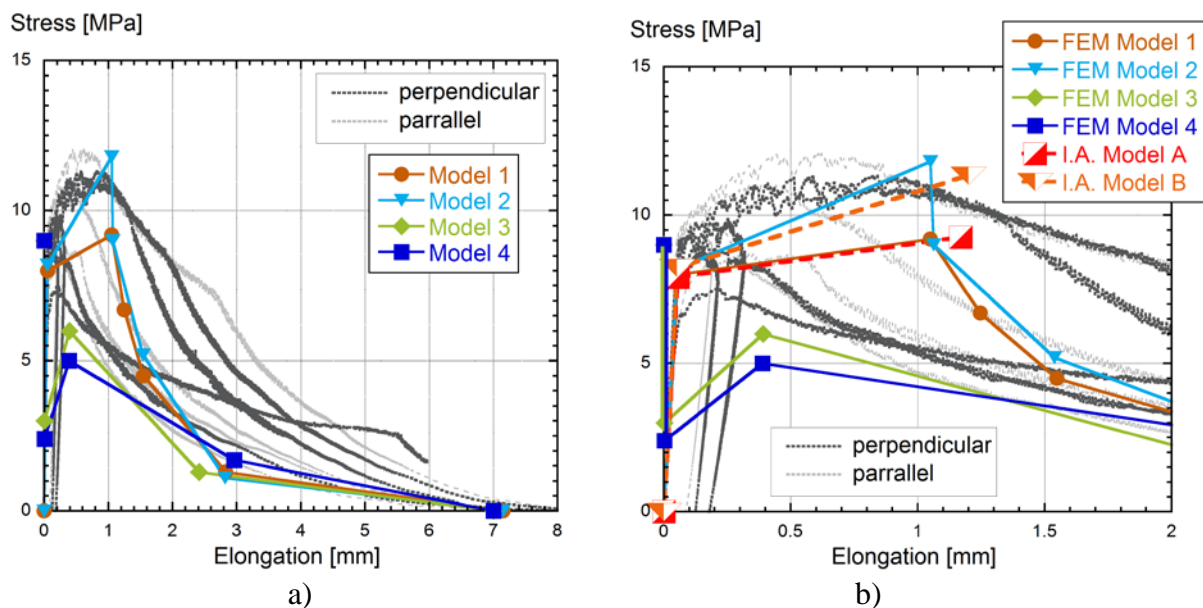

a)   b)

Figure 7: Tensile response: experimental results vs models: a) overview with FEM models, b) close up on peak range, with results of inverse analysis method: I.A. Models A and B. <u>NB:</u> measurement basis of LVDT $l_{mes,2}$=280 mm.

4. CONCLUSIONS

- A new method has been proposed for the objective determination of the elastic limit of UHPFRC from 4 PT bending tests. This method was validated by comparison with direct tensile test results and FEM models of similar specimen.
- An original analytical inverse analysis method extending models from [6, 8] has been applied successfully to the determination of the tensile properties of strain hardening UHPFRC from the Chillon Viaduct site.
- The material properties determined experimentally and by inverse analyses clearly indicate that the UHPFRC cast on the Chillon site exhibits in-place a strain hardening response and fulfills all requirements regarding the tensile properties.

REFERENCES

[1] Kanakubo, T., 'Tensile characteristics evaluation method for ductile fiber-reinforced cementitious composites', Journal of Advanced Concrete Technology, **4** (1) (2006) 3-17.

[2] Oesterlee, C., 'Structural Response of Reinforced UHPFRC and RC Composite Members'. Doctoral thesis n° 4848, 2015, Ecole Polytechnique Fédérale de Lausanne.

[3] Maya Duque, L.F. and Graybeal, B., 'Fiber orientation distribution and tensile mechanical response in UHPFRC'. *Materials and Structures*, **50** (1) (2016) 55.

[4] Wille, K., Tue, N.V., and Parra-Montesinos, G.J., 'Fiber distribution and orientation in UHP-FRC beams and their effect on backward analysis'. *Materials and Structures*, **47** (11) (2014) 1825-1838.

[5] Bastien-Masse M., Denarié E., Brühwiler E., 'Effect of fiber orientation on the in-plane tensile response of UHPFRC reinforcement layers', *Cement and Concrete Composites*, **67** (2016) 111-125.

[6] AFGC, 'Bétons Fibrés à Ultra Hautes Performances', Recommandations, Edition révisée, Association Française de Génie Civil, 2013, Paris.

[7] SIA 2052:2016, 'Béton fibré ultra-performant (BFUP): Matériaux, dimensionnement et exécution', Cahier technique SIA 2052, (2016), SNR 592052:2016 fr, Zürich.

[8] Rigaud, S., Chanvillard, G., and Chen, J., 'Characterization of Bending and Tensile Behavior of Ultra-High Performance Concrete Containing Glass Fibers', Proceedings HPFRCC 6, Springer Netherlands: Dordrecht, 2012, 373-380.

[9] Chanvillard, G., Corvez, D. 'Explicit back analysis method for quick determination of direct tensile strength of plate structural members'. in F. Toutlemonde and J. Resplendino Proceedings UHPFRC 2013, 2nd International Symposium on Ultra-High Performance Fibre-Reinforced Concrete, (UHPFRC). 2013. Marseille. RILEM Pro 87, 659-668.

[10] Baby, F., Graybeal, B., Marchand, P., and Toutlemonde, F., 'UHPFRC tensile behavior characterization: inverse analysis of four-point bending test results'. Materials and Structures, 46 (8) (2013) 1337-1354.

[11] López, J.Á., Serna, P., Navarro-Gregori, J., and Camacho, E., 'An inverse analysis method based on deflection to curvature transformation to determine the tensile properties of UHPFRC'. Materials and Structures, 48 (11) (2015) 3703-3718.

[12] Wuest, John, 'Comportement structural des Bétons de Fibres Ultra Performants (BFUP) en traction dans des éléments composés', thèse n° 3987, 2007, Ecole Polytechnique Fédérale de Lausanne.

[13] Denarié, E., 'Essais de caractérisation-réponse en traction', Actes de la 2ème journée d'étude du 22 octobre 2015: Béton fibré ultra-performant-Concevoir, dimensionner, construire. HEIA Fribourg and Berner Fachhochschule, 2015, 25-36.

[14] Denarié, E., Brühwiler, E., 'Cast-on site UHPFRC for improvement of existing structures – achievements over the last 10 years in practice and research', Proceedings HPFRCC7, 1-3 June 2015, Stuttgart, Germany, 473-480.

[15] Brühwiler, E., Bastien-Masse, M., Mühlberg, H., Houriet, B., Fleury, B., Cuennet, S., Schär, P., Boudry, F., Maurer, M., 'Strengthening the Chillon viaducts deck slabs with reinforced UHPFRC'. IABSE Symposium Report **105** (24) (2015) 1-8.

[16] Bernardi, S., Jacomo, D., Boudry, F., 'Overlay Ductal®: a durable solution for bridges retrofitting', 1st International Interactive Symposium on UHPC, Des Moines, Iowa, 2016.

[17] Neuber H., "Der zugbeanspruchte Flachstab mit optimalem Querschnittsübergang". *Forschung im Ingenieurwesen*, **35** (1) (1969) 29–30.

[18] FEM Code MLS, ver. 8.6.1, FEMMASSE, http://www.femmasse.com/, The Netherlands, 2006.

[19] Sadouki H., Denarié E., 'Modelling of UHPFRC in composite structures', Deliverable D26, European project SAMARIS, http://www.fehrl.org/?m=32&id_directory=356, 2006.